D8

LASER ANEMOMETRY FOR HOT SECTION APPLICATIONS

Richard G. Seasholtz, Lawrence G. Oberle, and Donald H. Weikle
National Aeronautics and Space Administration
Lewis Research Center

INTRODUCTION

The objective of this in-house program is to develop laser anemometers (LA's) for use in the study of the hot section components of turbomachinery. Specifically, laser anemometers are being developed for use in the 50.8-cm (20-in.) diameter warm turbine and high-pressure turbine (HPT) facilities at Lewis. This paper presents a brief review of the status of the program along with some preliminary data taken in an open-jet burner.

A stepwise approach is being followed which builds on the experience gained in the development of laser anemometer systems for cold-flow turbomachinery facilities (refs. 1 and 2). The procedure being followed for the development of the hot section laser anemometer systems is

(1) establish measurement objectives for each facility--parameters to be measured and accuracies
(2) develop an analytical model for the complete LA systems
(3) perform necessary experiments to provide data not otherwise available; e.g., seed properties, surface relectivity, and window contamination
(4) experimentally verify the model using the open-jet burner facility
(5) optimize LA system design to give desired accuracies in minimum run time.

MEASUREMENT OBJECTIVES

The measurement objectives for both the warm turbine and the high pressure turbine facilities are to measure the following parameters with the given accuracies: mean velocity, 1 percent; flow angle, 1°; turbulence intensity, 10 percent; and turbulence scale, 20 percent. Also, it is desirable that these measurements be made to within 2 mm of the end walls. Finally, because of the high cost of operating these facilities, the LA systems must be designed to take these data in a minimum of experimental run time.

OPEN JET BURNER

An open-jet burner facility is being used as a test bed for the development and testing of all components of the laser anemometer system--optics, traversing hardware, seed generators, and windows. Furthermore, the extensive software needed for control and data acquisition will be written and tested in this facility before the system is installed in the turbine facilities, thus minimizing the amount of expensive debugging in the turbine facilities.

The open-jet burner facility consists of a general purpose laboratory combustor (fig. 1) and associated controls. The mixing and flow in this combustor closely approximate those of many conventional gas turbine combustors and the critical features of the combustion chemistry are reproduced. The

fuel (Jet A) is introduced at the front of the combustor by a pressure atomizing fuel nozzle. The combustion is stabilized in the forward section of the combustor by developing a strong, swirl stabilized recirculation zone. The hot combustion gases are cooled by dilution jets which are located at the back of the combustor. The primary and secondary jets have independent air supplies to permit adjustment of the velocity and temperature profiles at the exit. The ignitor, a flame monitor, and instrumentation ports are mounted in an instrumentation ring located between the primary and secondary sections. Seed particles are introduced through a tube mounted in one of the instrumentation ports. The 50.8-mm (2-in.) diameter exhaust can be operated over a temperature range of 1000 to 1600 K (1300° to 2500° F) at Mach numbers of 0.2 to 0.8.

OPTICAL CONFIGURATION

Several types of optical designs are being considered. The primary design is a conventional single component dual-beam fringe-type configuration as illustrated in figure 2. The other types of laser anemometers under consideration are

(1) a two-spot time-of-flight LA, which offers the ability to measure smaller particles than a fringe LA but suffers from low data rates in highly turbulent flow.

(2) a new design time-of-flight system developed under Grant NAS 3-2 at Case Western Reserve University (ref. 3). This configuration using four elliptical spots should give data rates similiar to a fringe system, but should be significantly more sensitive.

To illustrate the effect that various optical system parameters have on the performance of a fringe-type LA we can write the expression for the lower bound of the variance of the velocity measurement for a single particle (ref. 4) as

$$\sigma_{mv}^2 = \frac{8}{\pi^{1/2}} \left(\frac{hc}{\eta\lambda\sigma\Omega}\right) \frac{\Gamma_o}{P^2} \frac{v^3 w_o^3}{N^2 + 18/\pi^2} \tag{1}$$

where Γ_o represents the background light flux; v, the velocity; $2w_o$, the diameter of the probe volume; P, the laser power; N, the number of fringes; h, Planck's constant; c, the velocity of light; λ, the wavelength of the laser light; η, the quantum efficiency of the photodetector; Ω, the solid angle of the light collection optics; and σ, the light-scattering cross section of the particle. Equation (1) shows that to reduce the error for a given measurement it is desirable to

(1) have particles with a large light-scattering cross section (yet small and light enough to follow the flow, (e.g. about 1 micrometer diameter for most turbomachinery flows)

(2) have small f number optics (i.e. larger Ω)that captures as much of the light scattered from the particle as possible

(3) have a small probe volume with many fringes

(4) minimize the amount of stray background light (flare)

Note that the fringe spacing for a given velocity is constrained by the frequency responses of the photodetector and the signal processor (typically about 200 MHz). For example, with a 500-m/sec flow velocity resulting in a

150-MHz Doppler frequency, the fringe spacing is $v/f = 3.3$ micrometers. The minimum probe volume diameter $2w_0$ is then set by the number of cycles required by the signal processor. If 10 cycles are required, the minimum probe volume diameter would be 33 micrometers for this example.

The final focusing lens is a critical element of the optical system because it not only determines the minimum size of the probe volume, but it also determines how well the scattered light can be focused at the field stop. The field stop (a pinhole aperture usually located in front of the photodetector) acts as a spatial filter that prevents light scattered from surfaces near the probe volume (flare) from reaching the photodetector, thus reducing the r_0 term in equation (1). This ultimately determines how close to the end walls and blades that measurements can be made. The lens selected for the warm turbine system is a three-element, air-spaced, f/2.5 design, with a 100-mm clear aperture and a 235-mm back focal length.

Another consideration in determining the time required to measure turbulent flow parameters to the required accuracy is that velocity measurements taken within the correlation time of the flow are not independent. As shown in reference 5 the variance in the measurement of the mean velocity is

$$\sigma^2_{\overline{mv}} = \frac{2\tau_c}{T}\left[\frac{\sigma^2_{mv}}{2R\tau_c} + \sigma^2_v\left(1 + \frac{1}{2R\tau_c}\right)\right] \qquad (2)$$

where σ^2_{mv} is the variance of the individual particle velocity measurements (given by eq. (1)), T is the time over which the data is acquired, R is the mean data rate, σ^2_v is the variance of the flow fluctuations (the square of turbulence intensity), and τ_c is the flow correlation time. Thus, in addition to the data rate, the time scale and turbulence intensity of the flow must be known in order to estimate the data acquisition time. Note that increasing the data rate will not necessarily reduce the data acquisition time.

The selection of the type of optical configuration will be based on experimental evaluations to be made in the open-jet burner facility. The time required to measure the flow parameters given in the Measurement Objectives section along with the minimum distance that these measurements can be made from solid surfaces are the criteria that will be used to select the optical configuration.

TRAVERSING SYSTEM

The traversing system for the open jet burner facility is constructed using standard, commercially available linear actuators for XYZ motion of the optics package. A similar traversing system has been designed for the warm turbine system. A two-axis goniometer stage will be used to position a mirror located after the final focusing lens. This will permit the optical axis to be pointed along a radial line as well as slightly off the radial line to minimize shadowing caused by the shape of the turbine blades. A commercial controller is to be used for the actuators of the traversing systems; both local control and remote computer control via an RS-232 serial interface are available.

SEED PARTICLES

Particle characteristics necessary for hot section laser anemometry are primarily the same as ambient temperature laser anemometry with the exception that hot section particles must retain those characteristics at the high temperatures. A selected grade of alumina sized at 1.0 micrometer is being used initially. Other particles on hand for later trials are titanium dioxide, silicon carbide, hollow phenolic spheres, and Georgia clay.

A commercial aerodynamic particle sizing system is being used to presample the particles in use before a test and will be used to sample the exhaust products. This system consists of the particle sizer (ref. 6) along with a microcomputer, disk drive, and printer. The included software for this system is sufficient to analyze and graphically portray all the needed information on particles in the size range that we are using. The system can easily be calibrated with a selection of known particles. Samples of the alumina have been taken with the particle sizing system and the size distribution looks good for our use (fig. 3). No samples of this material have yet been acquired after going through the burner.

The particle generation system consists of a commercial, high volume, fluidized bed generator (ref. 7) as shown in figure 4. This system was selected so that we could be assured of high particle concentrations for present and future known applications. This system operates by injecting the alumina or other particles into a bed of brass beads (approx. diam 100 micrometers). As the bed of beads is fluidized and mixed the particles are deagglomerated and ejected from a 20-mm diameter nozzle.

Since we are restricted in the diameter of a penetration into the burner, we cannot achieve a sufficient flow rate to fluidize the brass beads without bypassing some of the particles. The concentration is sufficient using a 3-mm inlet into the burner when the particle generator is operating properly. We have had clogging problems and two failures in the mixer in approximately 40 hr of usage. The clogging problem may be caused by moisture in the alumina.

A seed injection probe has been designed for the warm turbine that can be remotely moved in the radial and circumferential directions. The range of movement of the seed injection probe takes into account the large turning angle (75°) of the stator.

WINDOWS

Gaining optical access to the stator and rotor passages of a turbine without modifying the flow is a challenging design problem even for cold flow at low pressures. The warm turbine facility will use two windows. One will cover the stator passage and the other the rotor passage. Only one window will be installed at a time. Each window will be curved to match the tip radius and will be mounted flush with the inside surface so the flow will not be disturbed. The window material is synthetic sapphire, selected for its strength at high temperature and good optical properties. Because of their curvature the windows will act as cylindrical lenses; the aberration introduced is minimized by making the windows relatively thin (about 3 mm). Compensating optics will be used to correct the remaining aberration.

One of the major concerns in the design of the LA for the turbine facilities is the unknown rate of contamination of the windows. It is expected that combustion products, lubricating oil, and seed material will be deposited on the window. Tests are being conducted in the open-jet burner facility to establish the contamination rate. Various means of keeping the window clean, such as using an air purge, will be examined. Window cleaning procedures will be studied to determine a practical means of cleaning the window without removing it from the turbine. A sapphire test window has been mounted on the traversing table and we will be watching the change in data rate during burner startup and as a function of time at various distances from the hot gases. The window will be examined after exposure to determine the type of contaminants. The type of contaminants and rate of buildup data can then be used to determine if a high-temperature, on-line window cleaning method is necessary and possible.

DATA PROCESSING AND EXPERIMENT CONTROL

In the laser anemometry program the computer has become a necessary tool, chiefly due to the requirement that data be obtained at rates exceeding 5 kHz and that the data be reduced, at least partially, on line. In addition to the data acquisition requirements, the computer will become the experiment controller, performing such housekeeping procedures as deciding when to move the optics into position, moving the optics, how long to take data, and which data to keep.

In order to meet these requirements, a computer with a large memory, a fast mass storage device, and control capabilities was purchased. The computer, a PDP 11/44, is now installed in the open-jet burner facility. Using the RSX-11M multitasking operating system, the PDP 11/44 will be able to run several on-line programs 'simultaneously': acquiring data, reducing and storing the acquired data, and presenting a preliminary data summary. In addition to the data acquisition and experiment control functions, the PDP 11/44 will be able to produce high quality on-line graphics, both on the terminal and on a graphics printer. A block diagram of this computer system is shown in figure 5.

Until the PDP 11/44 is operational, a small laboratory minicomputer is being used to take data with a program which controls the traversing system, takes up to 4000 data points, and draws a frequency (or velocity) histogram of the acquired data (figs. 6(a) and 6(d)). The data comes in from a counter-type signal processor, on a direct memory access (DMA) line, and is stored in memory as two 16-bit words per data point. The time-of-flight through the required number of fringes (time data) and the time between the present and most recent data point (TBD data) are both converted to a FORTRAN readable form. If desired, this data can then be stored on disk. Finally the program performs the necessary calculations to plot a frequency histogram.

Even though the on-line data reduction provides a measure of the average data rate, in order to properly evaluate the autocorrelation outputs (figs. 6(c) and 6(f)) a probability histogram of the time between data points is necessary (figs. 6(b) and 6(e)). Because the flow is randomly time-sampled, data points must occur relatively close together temporally (and therefore spatially) for the autocorrelation to be meaningful. If this occurs, as shown in both examples, data can then be autocorrelated to obtain a measure of the

turbulence scale. (The autocorrelation is calculated using the procedure given in ref. 8.) The data shown in figures 6(a) to (c) were taken in the potential core of a small air jet (turbulence intensity about 1.6 percent) and the data in figures 6(d) to (f) were taken in the mixing region of the open jet burner exhaust (cold flow), which had a much higher turbulence intensity (about 30 percent).

The on-line program has recently been modified to take velocity surveys; that is, to move the optics under program control, take data, and plot a profile of the velocity component chosen by the experimenter. Examples of radial surveys of mean axial velocity and turbulence intensity taken in the exhaust of the open-jet burner are shown in figure 7(a) for cold flow and figure 7(b) for hot flow.

Future modifications will allow the program to take data between the blades of a rotating turbine, and keep track of not only the position of the optics, but also the position of the turbine rotor with reference to a fixed point.

PLANS

We plan to install the laser anemometer system in the warm turbine facility during 1984 and make it operational in early 1985. Preliminary design work for the high-pressure turbine facility (HPT) window is now underway.

REFERENCES

1. Goldman, L. J. and Seasholtz, R. G., "Laser Anemometer Measurements in an Annular Cascade of Core Turbine Vanes and Comparison with Theory," NASA TP-2018, 1982.
2. Powell, J. A., Strazisar, A. J. and Seasholtz, R. G., "High-Speed Laser Anemometer System for Intrarotor Flow Mapping in Turbomachinery," NASA TP-2018, 1982.
3. Edwards, R. V., "Laser Anemometer Optimization," Presented at Turbine Engine Hot Section Technology (HOST) Workshop, NASA TM-83022, Cleveland, Ohio, October 19-20, 1982.
4. Lading, L., "The Time-of-Flight verses the LDA," Proceedings of the Third International Workshop on Laser Velocimetry, Purdue University, 1978.
5. Edwards, R. V. and Jensen, A. S., "Particle Sampling Statistics in Laser Anemometers: Sample and Hold Systems and Saturable Systems," J. Fluid Mech., vol. 133, 1983, pp. 397-411.
6. TSI, Inc. Model APS 33 Aerodynamic Particle Sizer Instruction Manual.
7. TSI, Inc. Model 9310 Fluidized Bed Aerosol Generator Instruction Manual, p. 2.
8. Smith, D. M. and Meadows, D. M., "Power Spectra from Random-Time Samples for Turbulence Measurements with a Laser Velocimeter," Proceedings of the Second International Workshop on Laser Velocimetry, Vol. 1, H. D. Thompson and W. H. Stevenson, eds., Bull. No. 144, Purdue Univ., 1974, pp. 27-44.

LABORATORY COMBUSTOR

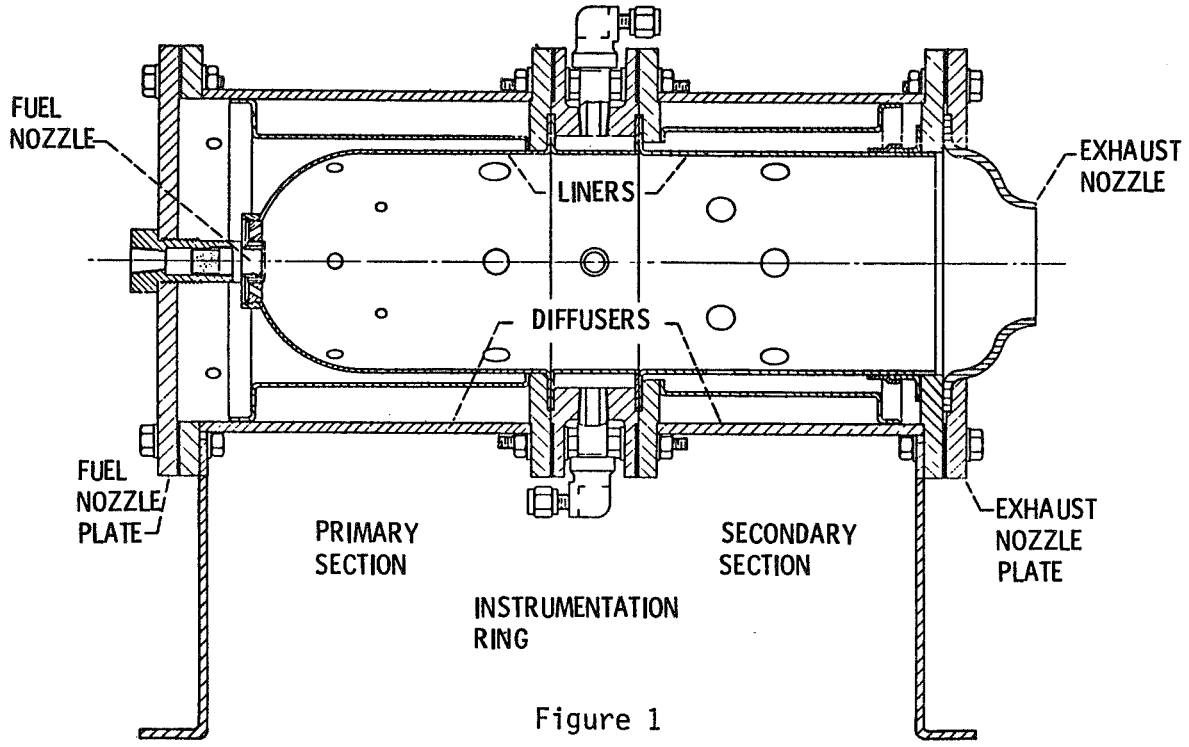

Figure 1

DUAL-BEAM FRINGE-TYPE LASER ANEMOMETER

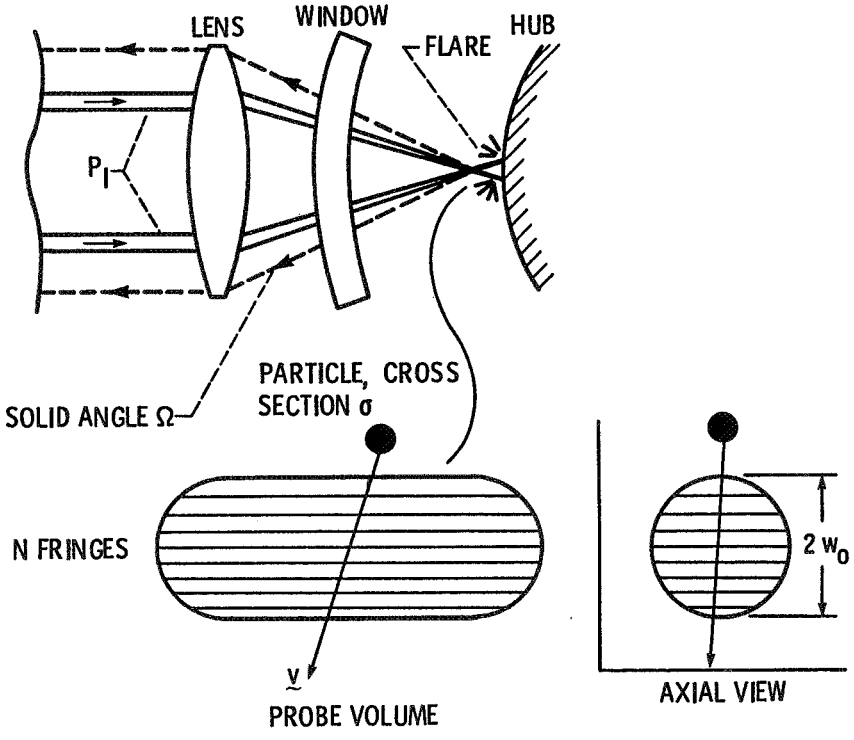

Figure 2

SIZE DISTRIBUTION OF ALUMINA POWDER

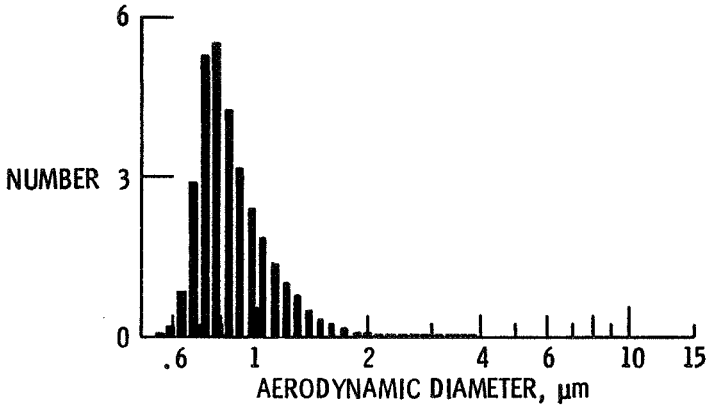

Figure 3

FLUIDIZED BED PARTICLE GENERATOR

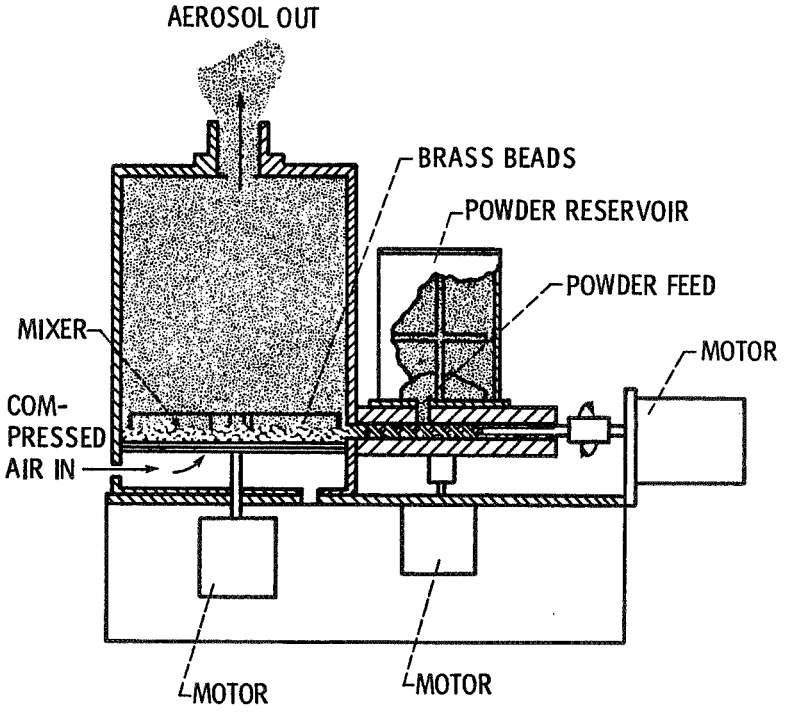

Figure 4

HOST LASER ANEMOMETRY SYSTEM

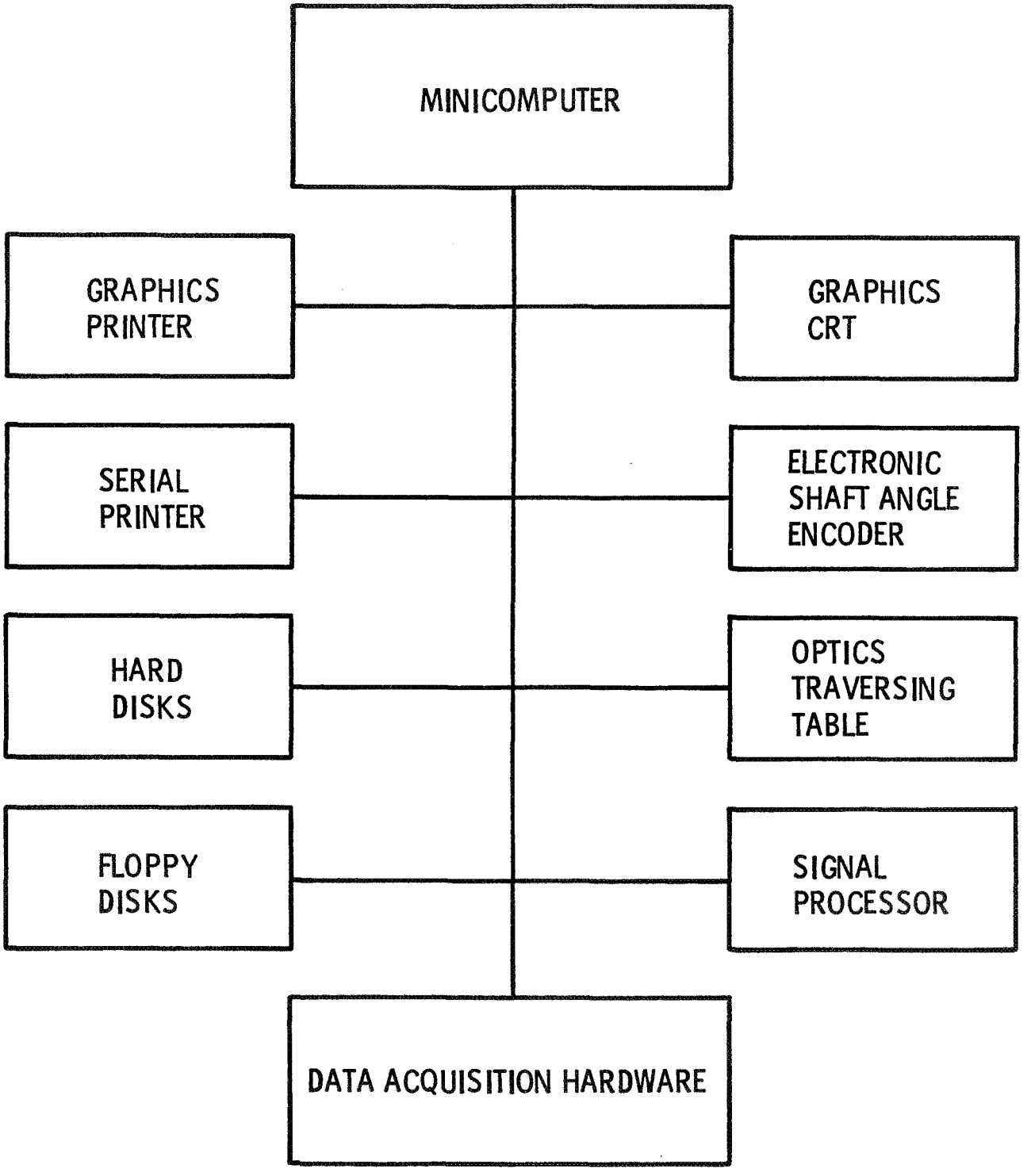

Figure 5

CRT DISPLAYS

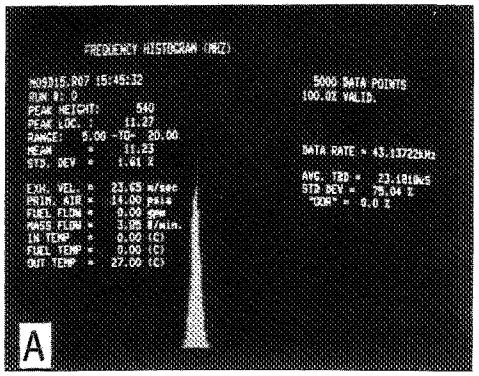

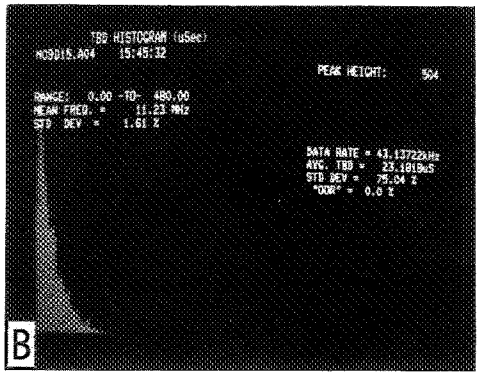

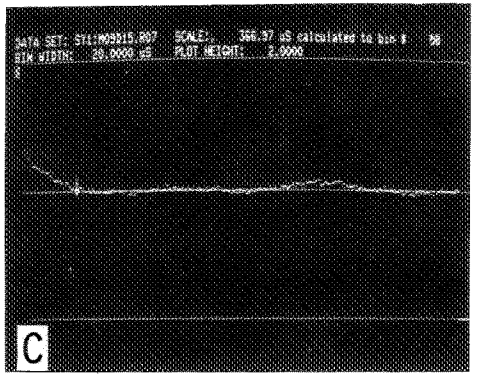

(A-C) LOW TURBULENCE CASE

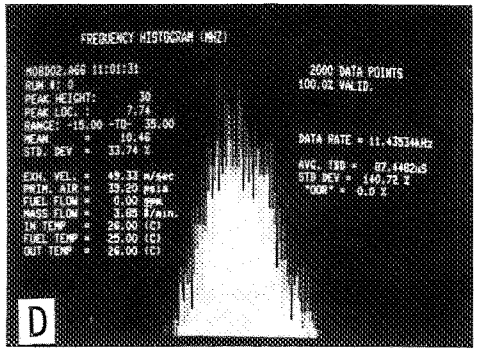

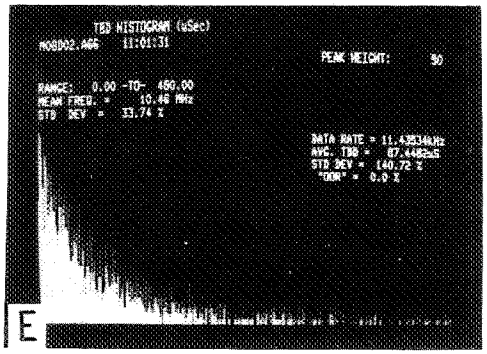

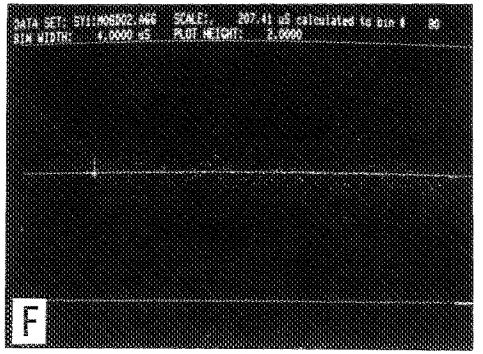

(D-F) HIGH TURBULENCE CASE

CS-83-2951

Figure 6

MEAN AXIAL VELOCITY AND TURBULENCE INTENSITY

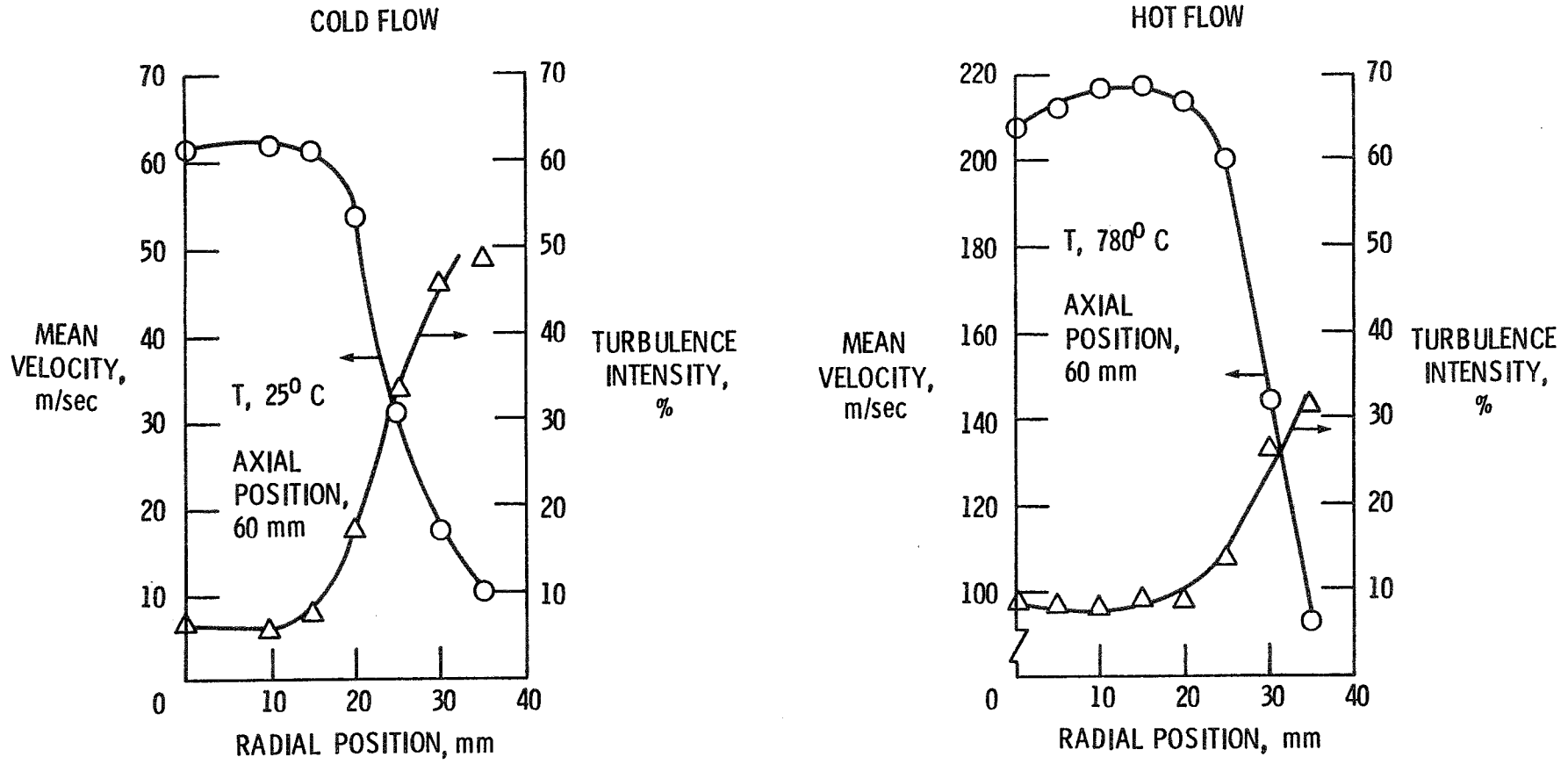

Figure 7